# Two-temperature frequency-dependent electrical resistivity in solid density plasmas produced by ultrashort laser pulses

R. Cauble
*Lawrence Livermore National Laboratory, Livermore, California 94550*

W. Rozmus
*Department of Physics, University of Alberta, Edmonton, Alberta, Canada T6G 2J1*
(Received 9 March 1995)

A model of the plasma resistivity, or equivalently the electron-ion collision frequency $\nu$, which can be used to describe absorption of ultrashort laser pulses in solid density plasmas has been constructed. Using kinetic theory based on a memory function formulation and a projection operator method, we have derived an analytical expression for $\nu$, which is valid in strongly coupled plasmas, properly accounts for the laser frequency dependence, and can be applied to plasmas with different electron and ion temperatures.

PACS number(s): 52.25.Fi, 52.20.Fs

## I. INTRODUCTION

Transport theory of strongly coupled plasmas plays an important role in the understanding of physical properties of matter under extreme conditions found in astrophysical objects and laboratory experiments. In recent years, rapid development of technology related to the generation of ultrashort laser pulses has led to a number of innovative experiments [1] examining basic properties of solid density plasmas on time scales short ($<1$ ps) compared to the hydrodynamic expansion time. When subpicosecond laser pulses are focused on a solid target, the absorbed energy is conducted away by the cold matter underlying the absorption region, which is a skin depth (a few hundred angstroms in extent). Solid density plasmas thus created by ultrashort laser pulses can possess low temperatures (less than 100 eV) and be strongly coupled with respect to particle-particle interactions [2]. An important part of the absorption process is related to inverse bremsstrahlung, which in turn is completely described by the electrical resistivity incorporating the electron-ion collision frequency. Thus the knowledge of plasma transport properties is central to the problem of laser pulse absorption. Because of high densities where absorption takes place, the transport model must account for the strongly coupled nature of the plasma. In addition, since the laser light is absorbed at a specific frequency, the transport coefficients resulting from the model must incorporate this effect, i.e., the electrical resistivity must include proper dependence on a laser frequency. Moreover, simulations have predicted that the plasma may not be in equilibrium for much of the absorption time, i.e., the electron and ion temperatures may be very different [3,4]. Typically the electron temperature is higher. In addition to nonequilibrium within the absorption time, it has been shown that hydrodynamics cannot be ignored. Dharma-Wardana and Perrot, who employ density functional theory in a quantum mechanical calculation, have noted that the inclusion of time-dependence and two-temperatures may be necessary in order to describe many short pulse experiments [5]. Ng *et al.* have observed that even for pulse lengths of a few hundred femtoseconds, hydrodynamic modeling is required for proper interpretation of experimental results [6]. As a practical matter, in order to describe inverse bremsstrahlung in a hydrodynamics code, it is convenient, and often necessary, that values for the electrical resistivity be easy to calculate; an analytic formulation is, of course, preferred. Thus three fundamental issues—strong coupling, time dependence, and nonequilibria, and one practical issue—ease and generality of calculation must be addressed when describing absorption in short pulse laser interactions with solids. We have constructed a transport model [7–9] for strongly coupled plasmas which has given results consistent with experimental observations [10] and compared well with the results of numerical simulations [11] as well as other theories. The model is based on a memory function kinetic formulation and solved by a projection operator method in momentum space [7]. The derived transport coefficients are expressed in terms of static correlation functions and interparticle potentials. In particular, the choice of analytic potentials and correlation functions may allow the derivation of transport coefficients which are themselves analytic. Here, we have extended this model [7] to explicitly include frequency dependence. We have also introduced two-temperature correlation functions and interparticle potentials. The solution is a two-temperature ac electrical resistivity $\rho(\omega)$ suitable for use in a strongly coupled plasma. Because of simple functions incorporated into the model, $\rho(\omega)$ can be presented in an analytic form. In the following section we summarize the theoretical model and approximations involved in deriving $\rho(\omega)$. An explicit expression for $\rho(\omega)$ for two temperatures is shown in Sec. III. Section IV contains numerical results, comparison, and discussion.

 

## II. THEORETICAL MODEL

The starting point for the calculation of transport coefficients in strongly coupled plasmas is a kinetic model which has been described previously [7]. We summarize below the procedure which allows the solution of a kinetic equation by the moment expansion method, and then describe extensions to the model to account for both different electron and ion temperatures and frequency-dependent effects. As we show in Sec. III both effects significantly modify the transport coefficients and are particularly important in ultrashort pulse laser produced plasmas. The starting point for the calculation is the equilibrium averaged phase space density correlation function,

$$C(1,2;t)=\left\langle \left[ \sum_{j=1}^{N_{\alpha_1}} \delta(\vec{r}_1-\vec{r}_j^{\,\alpha_1}(t))\delta(\vec{p}_1-\vec{p}_j^{\,\alpha_1}(t))-n_{\alpha_1}f_M^{\alpha_1}(\vec{p}_1) \right] \left[ \sum_{k=1}^{N_{\alpha_2}} \delta(\vec{r}_2-\vec{r}_i^{\,\alpha_2}(t))\delta(\vec{p}_2-\vec{p}_j^{\,\alpha_2}(t))-n_{\alpha_2}f_M^{\alpha_2}(\vec{p}_2) \right] \right\rangle , \tag{1}$$

where $1=(\vec{r}_1,\vec{p}_1,\alpha_1)$, $\alpha_1=e,i$ and $f_M^{\alpha_1}(\vec{p}_1)=(1/2\pi m_{\alpha_1}T_{\alpha_1})^{3/2}\exp(-p_1^2/2m_{\alpha_1}T_{\alpha_1})$ is the Maxwellian distribution function. We know $C(1,2,;t=0)\equiv\tilde{C}(1,2)$, which is one of the benefits of formulating kinetic description in terms of the equilibrium averaged correlation functions $C(1,2;t)$ as compared to using one particle nonequilibrium distribution function. $\tilde{C}(1,2)$ can be expressed in terms of the equilibrium correlation function $h^{\alpha_1\alpha_2}$

$$\tilde{C}(1,2)=\delta_{\alpha_1\alpha_2}\delta(\vec{r}_1-\vec{r}_2)\delta(\vec{p}_1-\vec{p}_2)n_{\alpha_1}f_M^{\alpha_1}(\vec{p}_1) +n_{\alpha_1}f_M^{\alpha_1}(\vec{p}_1)n_{\alpha_2}f_M^{\alpha_2}(\vec{p}_2)h^{\alpha_1\alpha_2}(\vec{r}_1-\vec{r}_2) . \tag{2}$$

The Fourier transformed $C(1,2;t)$,

$$C^{\alpha_1\alpha_2}(\vec{k},\vec{p}_1,\vec{p}_2;t)=\int d^3(r_1-r_2) \times\exp[-i\vec{k}\cdot(\vec{r}_1-\vec{r}_2)]C(1,2;t) , \tag{3}$$

satisfies an exact kinetic equation of the following form [12],

$$\frac{\partial}{\partial t}C^{\alpha_1\alpha_2}(\vec{k},\vec{p}_1,\vec{p}_2;t)-\sum_{\alpha_3}\int_0^\infty dt_1 d^3p_3\Phi_{\alpha_1\alpha_2}(\vec{k},\vec{p}_1,\vec{p}_3;t_1) \times C^{\alpha_3\alpha_2}(\vec{k},\vec{p}_3,\vec{p}_2;t-t_1)=0 . \tag{4}$$

The memory function $\Phi_{\alpha_1\alpha_2}(\vec{k},\vec{p}_1,\vec{p}_2;t)$ consists of three parts

$$\Phi_{\alpha_1\alpha_2}=\Phi^{\rm FP}_{\alpha_1\alpha_2}+\Phi^{\rm MF}_{\alpha_1\alpha_2}+\Phi^{C}_{\alpha_1\alpha_2} ,$$

namely, a free streaming term,

$$\Phi^{\rm FP}_{\alpha_1\alpha_2}=i(\vec{k}\cdot\vec{p}_1/m_{\alpha_1})\delta(\vec{p}_1-\vec{p}_2)\delta_{\alpha_1\alpha_2}\delta(t) ,$$

a mean field term,

$$\Phi^{\rm MF}_{\alpha_1\alpha_2}=-i(\vec{k}\cdot\vec{p}_1/m_{\alpha_1})n_{\alpha_1}f_M^{\alpha_1}(\vec{p}_1)C_D^{\alpha_1\alpha_2}(k)\delta(t) ,$$

and the time-dependent collision operator $\Phi^C$. Above, $C_D^{\alpha_1\alpha_2}$ is the direct correlation function. The form of the collision term $\Phi^C$ underpins the transport coefficients we will derive. Since $\Phi^C$ contains correlations of all order in the particle number, approximations must be made. One particular form due to Mazenko is the disconnected approximation [12,13]. This form of $\Phi^C$ rigorously "disconnects" two-particle functions from those of higher order, revealing $\Phi^C$ in terms of products of two-particle functions plus other terms and resulting in a form which is amenable to calculation. The disconnected approximation has been shown to be effective in describing properties of plasmas with strong coupling [8,13]. Employing this approximation, we obtain the operator form of $\Phi^C$ (cf. Eq. (12), Ref. [7])

$$i\Phi^C_{\alpha_1\alpha_2}(\vec{k},\vec{p}_1,\vec{p}_2;t)n_{\alpha_2}f_M^{\alpha_2}(\vec{p}_2)=-\frac{1}{2}T_e\sum_{\alpha_3\alpha_4}\int d^3p_3d^3p_4\int\frac{d^3l}{8\pi^3}C_D^{\alpha_1\alpha_4}(l)\vec{l}\cdot\frac{\partial}{\partial\vec{p}_1} \times\left[ V_l^{\alpha_2\alpha_3}\vec{l}\cdot\frac{\partial}{\partial\vec{p}_2}C^{\alpha_1\alpha_2}(\vec{k}-\vec{l},\vec{p}_1,\vec{p}_2;t)C^{\alpha_4\alpha_3}(\vec{l},\vec{p}_4,\vec{p}_3;t) +V_{k+l}^{\alpha_2\alpha_3}(\vec{k}-\vec{l})\cdot\frac{\partial}{\partial\vec{p}_2}C^{\alpha_1\alpha_3}(\vec{k}-\vec{l},\vec{p}_1,\vec{p}_2;t)C^{\alpha_4\alpha_2}(\vec{l},\vec{p}_4,\vec{p}_2;t) \right] . \tag{5}$$

In Eq. (5), $V_l^{\alpha_1\alpha_2}$ is the Fourier transform of the interparticle potential between species $\alpha_1$ and $\alpha_2$.

The kinetic Eq. (4) can be solved by expanding $C^{\alpha_1\alpha_2}(\vec{k},\vec{p}_1,\vec{p}_2;t)$ in moments of momentum (see, e.g., the monograph by R. Balescu [14], for a discussion of the moment expansion method). Equation (4) then reduces to the system of transport equations for hydrodynamic correlation functions. These equations have the form of

the Navier-Stokes equations; comparison of the two sets reveals the transport coefficients in terms of momentum moments of the collision operator [15,16]. The expansion can be easily carried out using a projection operator approach [7,14]. Choosing the Maxwellian as a natural weight function, one can use Hermite polynomials to construct an orthonormal set of momentum states. The projection operator $P$ contains those states describing hydrodynamics (conservation relations); the complementary operator $Q=I-P$ contains the remainder of the momentum states. A measure of the completeness of the solution is the number of states retained in $Q$. The hydrodynamic momentum states and a summary of the momentum expansion solution are given in the Appendix. Retaining only the first nonhydrodynamic state in $Q$ produces a solution which is equivalent to the Grad 13-moment solution to transport coefficients [17]. These are known [14] to be factors of 2–3 different from the classical results obtained by Braginskii [18] for weakly coupled systems; calculations like the one described herein are necessary for more highly coupled systems. In order to include most of this difference, it is necessary to also retain in $Q$ the next contributing state, which produces the equivalent of Grad's 21-moment solution. (For accuracies of a few percent, it is sufficient to stop here [14].) Using the projection operators $P$ [Eq. (A2)] and $Q$ [Eq. (A5)] on the Laplace transformed kinetic Eq. (4), reveals a system of transport equations having the following form:

$$(-iz-P\Phi P)PF^{\alpha_1\alpha_2}-P\Phi Q\frac{1}{-iz-Q\Phi Q}Q\Phi P\,PF^{\alpha_1\alpha_2}=Pn_{\alpha_1}f_M^{\alpha_1}S^{\alpha_1\alpha_2}(k)\ , \quad (6)$$

where,

$$F^{\alpha_1\alpha_2}=\int d^3p_2 C^{\alpha_1\alpha_2}(\vec{k},\vec{p}_1,\vec{p}_2;t)\ ,$$

and $S^{\alpha_1\alpha_2}(k)$ is the static structure factor. Comparing (6) with the Navier-Stokes equations reveals the transport coefficients in terms of combinations of matrix elements of memory functions.

## III. ELECTRICAL RESISTIVITY

We are interested in the momentum transfer between electrons and ions. By comparing Eq. (6) with the Navier-Stokes equations we can identify the friction coefficient $\xi$ proportional to the generalized collision frequency $\nu$

$$\xi=m_e n_e\nu$$
$$=m_e n_e(\langle H_p^e|i\Phi^C|H_p^e\rangle - \langle H_p^e|i\Phi^C Q[-iz+iQ\Phi^C Q]^{-1}Qi\Phi^C|H_p^e\rangle)\ , \quad (7)$$

where $|iH_p^e\rangle$ are the momentum states (the Appendix) and $z$ describes frequency dependence of the transport coefficient. Note that (7) reduces to the general dc result for $\xi$ [Eq. (28) from [7]] in the limit of $z\to 0$. From Eqs. (5) and (7), we see that in order to obtain the collision frequency $\nu$ and related electrical resistivity, we must specify the form of two body correlation function $C^{\alpha_1\alpha_2}(\vec{k},\vec{p}_1,\vec{p}_2;t)$. To do this rigorously would require the exact solution of the original kinetic equation, Eq. (1), so several approximations must be made.

The free particle form of $C^{\alpha_1\alpha_2}(\vec{k},\vec{p}_1,\vec{p}_2;t)$

$$C^{\alpha_1\alpha_2}(\vec{k},\vec{p}_1,\vec{p}_2;t)=i\int_C\frac{dz}{2\pi}e^{-izt}\frac{\tilde{C}(\vec{k},\vec{p}_1,\vec{p}_2)}{z-\vec{k}\cdot\vec{p}_1/m_{\alpha_1}} \quad (8)$$

is a solution of Eq. (4) with $\Phi^{MF}=\Phi^C=0$. Substituting Eq. (8) into (5) and taking the Markovian ($t=0$) and local ($\vec{k}=0$) limits, we obtain

$$i\Phi^C_{\alpha_1\alpha_2}(\vec{k}=0,\vec{p}_1,\vec{p}_2;t=0)n_{\alpha_2}f_M^{\alpha_2}(\vec{p}_2)$$
$$=-\tfrac{1}{2}T_e\sum_{\alpha_3\alpha_4}\int d^3p_3d^3p_4\pi\int\frac{d^3l}{8\pi^3}C_D^{\alpha_1\alpha_4}(l)V_l^{\alpha_2\alpha_3}\vec{l}\cdot\frac{\partial}{\partial\vec{p}_1}\delta(\vec{l}\cdot\vec{p}_4/m_{\alpha_4}-\vec{l}\cdot\vec{p}_1/m_{\alpha_1})$$
$$\times\vec{l}\cdot\frac{\partial}{\partial\vec{p}_2}[\tilde{C}^{\alpha_1\alpha_2}(\vec{l},\vec{p}_1,\vec{p}_2)\tilde{C}^{\alpha_4\alpha_3}(\vec{l},\vec{p}_4,\vec{p}_3)-\tilde{C}^{\alpha_1\alpha_3}(\vec{l},\vec{p}_1,\vec{p}_3)\tilde{C}^{\alpha_4\alpha_2}(\vec{l},\vec{p}_4,\vec{p}_2)]+(1\leftrightarrow 2)\ . \quad (9)$$

We will use Eq. (9) in calculations of the nonhydrodynamic moments in Eq. (7). Taking the Markovian limit of $\Phi^C$ is not inconsistent with using Eq. (7) to find a time-dependent result if (7) is applied in the overdense region, where the local plasma frequency $\omega_{pe}$ is higher than the laser frequency $\omega$. In subpicosecond laser-solid interactions, the dominant absorption indeed takes place in the overdense region.

Because of screening, the major contribution to the $l$ integration in Eq. (9) comes from the distances less than roughly a Debye length $k_D^{-1}$, i.e., for $l>k_D$. The Debye length is defined by

$$k_D^2=4\pi n_e e^2/T_e+4\pi n_i Z^2e^2/T_i\ . \quad (10)$$

Thus Eq. (8) will contribute to Eq. (9) only for $k>k_D$, or, setting $z=\omega$, when

$$\omega\geq\vec{k}\cdot\vec{p}_1/m_e\approx k_D(T_e/m_e)^{1/2}=\omega_{pe}\ . \quad (11)$$

Equation (11) is satisfied in underdense plasma; however, when $\omega_{pe}\gg\omega$, we can neglect $z$ compared to $\vec{k}\cdot\vec{p}_1/m_e$ in Eq. (8) and use the collisional memory function $\phi^C$ in the Markovian form (9). (In solid density aluminum irradiated by 800 nm light, for example, $\omega_{pe}/\omega\approx 10$.) Even when $\omega_{pe}\approx\omega$, including $\omega$ in (8) gives rise to only a 10% and

complicates the result, which we want to be analytic [9]. Inserting Eq. (8) into (9) and expanding the projection operators in Eq. (7) we obtain the ac collision frequency,

$$\nu(\omega)=M_{pp}-\frac{1}{D}[(-i\omega+M_{rr})M_{pq}^2+(-i\omega+M_{qq})M_{pr}^2 -2M_{pq}M_{pr}M_{qr}] , \quad (12)$$

where the momentum matrix elements $M$ are, except for the generalization to two temperatures, identical to Eqs. (36)–(41) of Ref. [7],

$$D=(-i\omega+M_{qq})(-i\omega+M_{rr})-M_{qr}^2 .$$

The matrix elements are defined in the Appendix. The dc collision frequency can be recovered from Eq. (7) by letting $\omega\rightarrow 0$. The corresponding expression for ac electrical resistivity is

$$\rho(\omega)=\frac{m_e}{e^2 n_e}\nu(\omega) . \quad (13)$$

The matrix elements Eqs. (A8) and thus $\nu$ in Eq. (12) are explicitly defined in terms of the following expressions which contain static correlations and two body potentials:

$$\Omega^{ee}=\int_0^\infty dk\, k^3 C_D^{ee}(k)[V_k^{ee}S^{ee}(k)+V_k^{ei}S^{ei}(k)] , \quad (14)$$

$$\Omega^{ei}=\int_0^\infty dk\, k^3 C_D^{ei}(k)[V_k^{ee}S^{ie}(k)+V_k^{ei}S^{ii}(k)] , \quad (15)$$

$$\Delta=\int_0^\infty dk\, k^3 C_D^{ei}(k)V_k^{ei}[S^{ee}(k)S^{ii}(k)-S^{ei}(k)S^{ie}(k)] . \quad (16)$$

To obtain explicit results, it now remains to choose the interparticle potentials and the static correlations which appear above. Recall that one motivation for this work is to obtain an expression for $\nu$ which has a simple enough form to be used inside hydrodynamics simulation codes. With this in mind, we choose the analytic Debye-Hückel (DH) form for the static correlations. While it may seem surprising that we employ weak coupling statics with the intention of retrieving a strong coupling result, comparison with more sophisticated static forms has shown that DH screening may be a reasonable approximation even for strongly coupled plasmas when the screening is applied inside a more complete theory [8,19]. This choice, while allowing a straightforward result, will introduce limitations when the coupling becomes very strong. This will be discussed in Sec. IV. The two-temperature Debye-Hückel total correlation functions can be written [20]

$$h^{\alpha_1\alpha_2}(k)=-(n_{\alpha_1}n_{\alpha_2})^{1/2}4\pi Z_{\alpha_1}Z_{\alpha_2}e^2\beta_{\alpha_1\alpha_2}\frac{1}{k^2+k_D^2} , \quad (17)$$

where $\alpha_1,\alpha_2=e,i,Z_{\alpha_i}$ is the charge of species $\alpha_i$, and $\beta_{\alpha_1\alpha_2}=1/T_{\alpha_1\alpha_2}$;

$$T_{\alpha_1\alpha_2}=\frac{m_{\alpha_1}T_{\alpha_2}+m_{\alpha_2}T_{\alpha_1}}{m_{\alpha_1}+m_{\alpha_2}} .$$

Neglecting terms of order $m_e/m_i$, the two-temperature direct correlation functions which we require are

$$C_D^{ei}=\frac{h^{ei}(k)}{L(k)} , \quad (18)$$

and

$$C_D^{ee}=\frac{1}{n_e}\frac{L(k)-S^{ii}(k)}{L(k)} , \quad (19)$$

where

$$L(k)=S^{ee}(k)S^{ei}(k)-S^{ei}(k)^2 . \quad (20)$$

Using Eq. (17) in Eqs. (18) and (19) we obtain

$$C_D^{ei}=4\pi Z_e^2\beta_{ei}\frac{k^2+k_D^2}{k^4+k^2k_D^2+Y} \quad (21)$$

and

$$C_D^{ee}=-4\pi\beta_{ei}\frac{k^2+k_{De}^2+Rk_{Di}^2}{k^4+k^2k_D^2+Y} , \quad (22)$$

where

$$k_{D\alpha_1}^2=4\pi Z_{\alpha_1}^2 n_{\alpha_1}e^2\beta_{\alpha_1} , \quad (23)$$

$$R=\frac{\beta_{ei}^2}{\beta_e\beta_i} , \quad (24)$$

$$Y=k_{De}^2k_{Di}^2(1-R) . \quad (25)$$

Above, $\beta_\alpha=1/T_\alpha$.

To complete the model, we use an extensively employed interaction potential [21], which, while having a Coulomblike form at moderate distances, is modified at short range to approximate quantum diffraction effects [7,11,19],

$$V^{\alpha_1\alpha_2}(r)=\frac{q_{\alpha_1}q_{\alpha_2}}{r}\left[1-\exp\left[\frac{-4}{\lambda_{\alpha_1\alpha_2}}\right]\right] , \quad (26)$$

where

$$\lambda_{\alpha_1\alpha_2}=\hbar/(2\pi\mu_{\alpha_1,\alpha_2}T_{\alpha_1\alpha_2})^{1/2} ; \quad (27)$$

$\mu_{\alpha_1\alpha_2}$ is the reduced mass. If Eqs. (18)–(26) are inserted into Eqs. (14)–(16), the latter equations can be solved analytically. By inserting these results into the matrix elements [Eqs. (A8)], analytic, though quite lengthy, expressions for the two-temperature ac electron-ion collision frequency $\nu$ (12) and electrical resistivity $\rho(\omega)$ (13) are obtained [22].

## IV. RESULTS AND DISCUSSION

In Fig. 1(a) we compare the single temperature dc electron-ion collision frequency $\nu$, Eq. (12), with the well-known model of Lee and More (LM) [23] as well as two versions of $\nu$ found from the Spitzer theory [24]. $\nu$ has been normalized to the electron plasma frequency, $\omega_{pe}$. The material is aluminum. The density is 2.7 g/cm$^3$, solid density. Temperatures up to 200 eV are considered. The LM model incorporates the results of several models

believed appropriate for distinct regions of density-temperature space. The curve labeled "NRL" is taken from Ref. [25]. The curve labeled "Spitzer" used the $\ln\Lambda$ prescription

$$\ln\Lambda=\tfrac{1}{2}\ln\left[1+\frac{b_{\max}^2}{b_{\min}^2}\right], \tag{28}$$

where $b_{\max}$ is the greater of the Debye length $k_D^{-1}$ and the ion sphere radius, $a=(4\pi n_i/3)^{-1/3}$ and $b_{\min}$ is the greater of the classical turning point, $\langle Z\rangle e^2/T_e$ and the thermal de Broglie wavelength (27). The ion charge $\langle Z\rangle$, taken from [26] is included on the right hand vertical scale.

As expected, the Spitzer-type models are not at all in agreement with the LM or our model. Each of these weak coupling formulations shows large disagreement with the models for solid density for temperatures less than about 400 eV. In general, the LM model predicts a larger $\nu$, and thus higher absorption, than our theory. The differences are difficult to reconcile as the two models are very different. For temperatures less than 6 eV (at solid density), the two models diverge. The coupling becomes too strong for our approximation of static correlations by their Debye forms. This limits our application of the model to temperatures greater than this value. Alternatively, the LM model is tied to a prescription thought to be accurate near the aluminum melting point. The

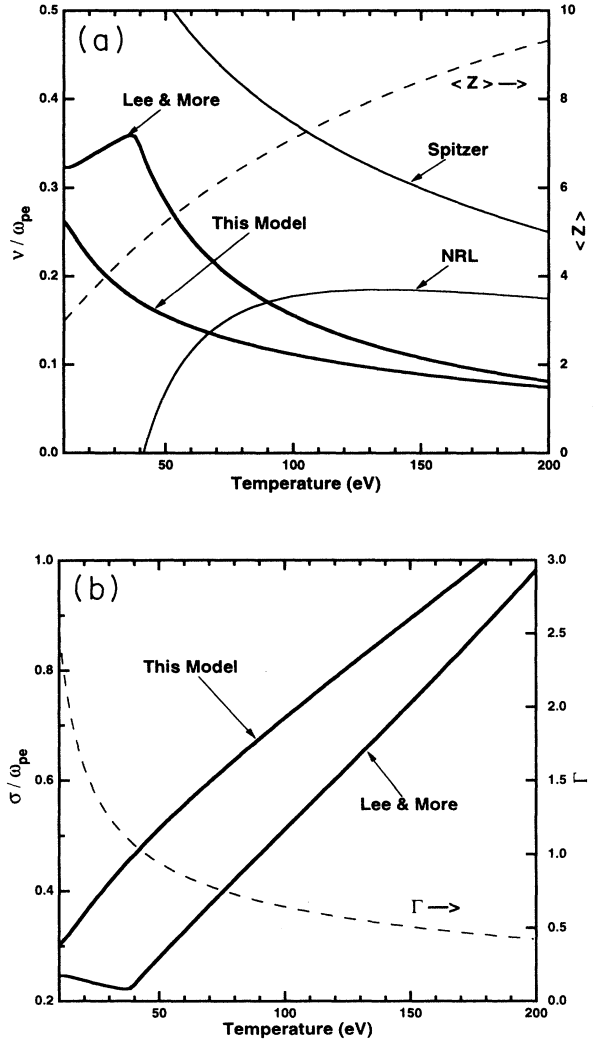


FIG. 1. (a) The single temperature ($T_i=T_e$), dc ($\omega=0$) electron-ion collision frequency $\nu$ from Eq. (12) in units of the electron plasma frequency $\omega_{pe}$ for solid density aluminum (2.7 g/cm$^3$) compared to the model of Lee and More [23]. A weak coupling model employing two different definitions of $\ln\Lambda$ is also plotted: "NRL" from the Naval Research Laboratory [25] and "Spitzer" from (28). The right hand vertical scale shows the values of average ionization $\langle Z\rangle$ used for all models. (b) The corresponding dc electrical conductivity (divided by $\omega_{pe}$). The right hand scale shows $\Gamma$, the ion-ion coupling parameter.

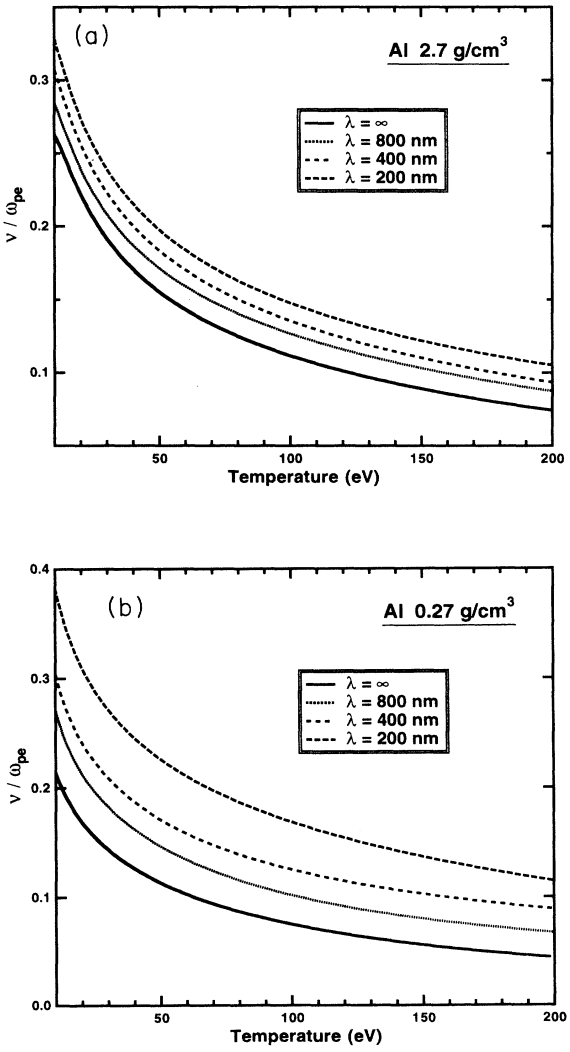


FIG. 2. (a) The single temperature ($T_i=T_e$) ac electron-collision frequency $\nu(\omega)$ from Eq. (12) in units of the electron plasma frequency for solid density aluminum (2.7 g/cm$^3$) for selected wavelengths. (b) Same as (a) but for one-tenth-solid density aluminum.

largest difference between our expression and LM (not quite a factor of two) occurs round 35 eV. The models are in better agreement near 10 eV and rapidly converge for higher temperatures. The dc electrical conductivity, $\sigma=\omega_{pe}^2/4\pi\nu$ is shown in Fig. 1(b). The ion-ion coupling parameter, $\Gamma=\langle Z\rangle^2 e^2/aT_i$ is given on the right hand scale. We note that a smaller $\nu$ than LM is consistent with some recent low intensity, low temperature absorption data [27].

In light absorption, allowing oscillations of the electrons in the presence of the radiation field within the limits set by the surrounding particles (via interparticle correlations) increases the collision rate and thus light absorption. This is shown by plotting ac collision frequency (12) in Fig. 2. In Fig. 2(a), the collision frequency, divided by $\omega_{pe}$ for solid density aluminum is shown as a function of temperature for several wavelengths. $\lambda=\infty$ is the dc rate. The plasma frequency $\omega_{pe}$ is about 4–20 times the laser frequency for these cases. The $\nu(\omega)$ increases as the frequency increases, but since $\omega/\omega_{pe}$ is relatively small, the increase is not dramatic. However, $\nu(\lambda=400$ nm) is about 20–25 % larger than the dc value, which can be important in describing absorption. Figure 2(b) shows the same information for aluminum at one-tenth-solid density. Here the fractional increase in $\nu$ is 30–50 %. Choosing 800 nm as a wavelength, $\nu(\omega)$ for several solid density materials is shown in Fig. 3. The results are dependent on the values of $\langle Z\rangle$. Interestingly, the range of $\nu(\omega)/\omega_{pe}$ is within a factor of two for most materials at solid density over a large range of temperatures. We have seen that the inclusion of dynamics can increase the rate of light absorption by near-solid density plasmas.

The two curves in Fig. 4(a) show $\nu(\lambda=\infty)/\omega_{pe}$ vs electron temperature in solid density aluminum for the single temperature case ($T_e=T_i$) and a two temperature example where $T_i$ is fixed at 10 eV. As the temperature disparity grows, so does the difference in collision rates and, thus, absorption. The reduction from the single temperature result is about 20% at 20 eV, 40% at 50 eV, and 55% at 100 eV. The reason for the reduction is increased screening. Screening of particles by other particles of the same kind (e.g., ions by ions) is governed mainly by the Debye length for those particles $k_{D\alpha}^{-1}$ where $\alpha=e,i$. However, electron-ion screening is determined by $k_D^{-1}$. The lower ion temperature dominates $k_D$ and thus determines the screening. The disparity is less significant at lower densities because, overall, screening is less important. Figure 4(b) shows the same curves for one-tenth density of solid aluminum. Figure 5 presents full ac two-temperature curves of $\nu(\omega)$ for solid density aluminum (a)

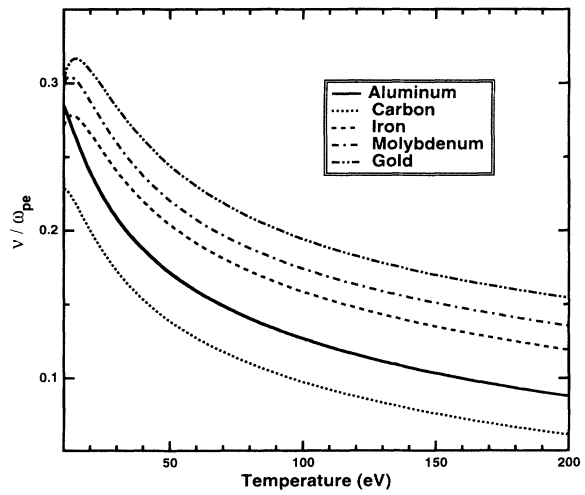


FIG. 3. The single temperature ($T_i=T_e$) ac electron-ion collision frequency $\nu(\omega)$ from Eq. (12) in units of the electron plasma frequency for selected solid density materials for a wavelength of 800 nm. For all cases $\omega_{pe}/\omega>10$.

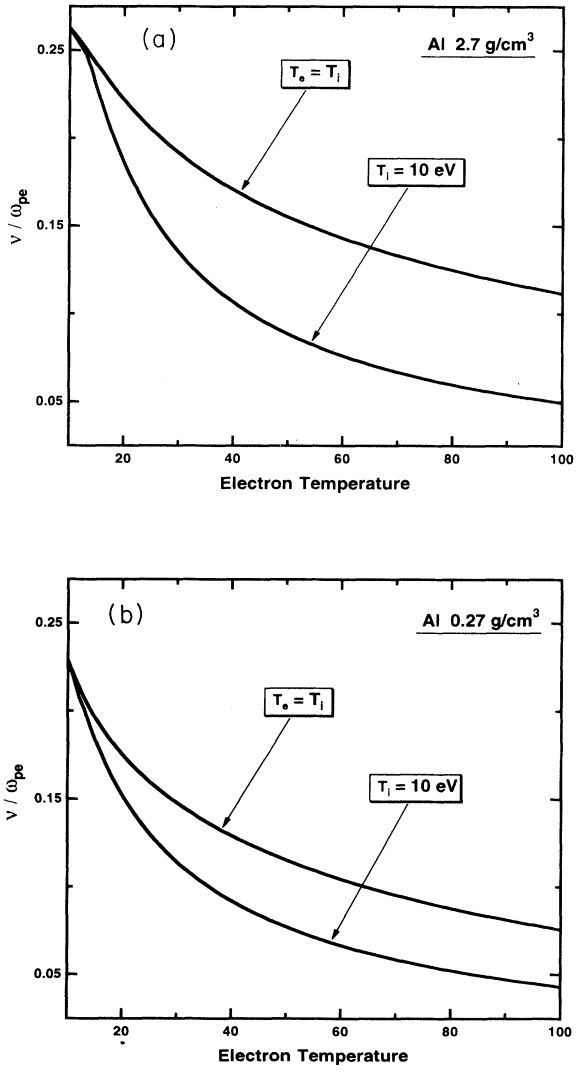


FIG. 4. (a) The two-temperature ac electron-ion collision frequency $\nu(\omega)$ from Eq. (12) in units of the electron plasma frequency for solid density aluminum at a wavelength of 800 nm as a function of electron temperature. The ion temperature is fixed at 10 eV. The single temperature calculation is included for comparison. (b) Same as (a) but for one-tenth-solid density aluminum.

and one-tenth-solid density aluminum (b). The ion temperature is fixed at 10 eV. In comparing the curves of different frequencies, the observations made above for the single temperature model (discussion of Fig. 2) can be repeated here. The higher the frequency, the greater the increase in the collision rate with roughly the same fractional change as with one temperature.

We have developed a model for the frequency dependent electron-ion collision rate in a strongly coupled, two component, two-temperature plasma. This is equivalent to the ac resistivity in such a system. The collision rate governs the inverse bremsstrahlung coefficient and thus the dominant absorption mechanism in ultrashort pulse laser interactions with solids. Emphasis in the model was placed in four areas: strong coupling, time dependence, two temperatures, and ease of use. Use of the disconnected approximation in the kinetic equation for time-dependent correlation functions assured a formalism which has given results for plasma transport coefficients in good agreement with computer simulations of strongly coupled systems [8,13]. The kinetic equation was formally solved by a projection operator method which incorporated sufficient number of terms so that the result is not subject to arbitrary multipliers based on weakly coupled systems. Time dependence was included by explicitly retaining frequency dependent terms in the solution. One approximation made at this juncture was to assume that $\omega_{pe} > \omega$, a situation normally obeyed in ultrashort pulse laser irradiation of solids. Nonequilibria were introduced with two-temperature static correlation functions. In order to produce an easily used, indeed analytic, result, the static correlations were approximated by their Debye forms and the bare interparticle potential by an approximate model potential [21]. This has the effect of limiting our results to $\Gamma < 3$ for aluminum. It was already known that weak coupling treatments of transport in strongly coupled plasmas would not provide estimates accurate enough for use in experiments or simulation codes [9,19,23]; see Fig. 1. We have shown quantitatively that inclusion of frequency dependence increases the resistivity, and thus absorption, by 20–50 % for wavelengths of short pulse lasers now operating. If the electron and ion temperatures are not in equilibrium, the rate will be reduced due to enhanced ion screening. This reduction can be as much as 50%.

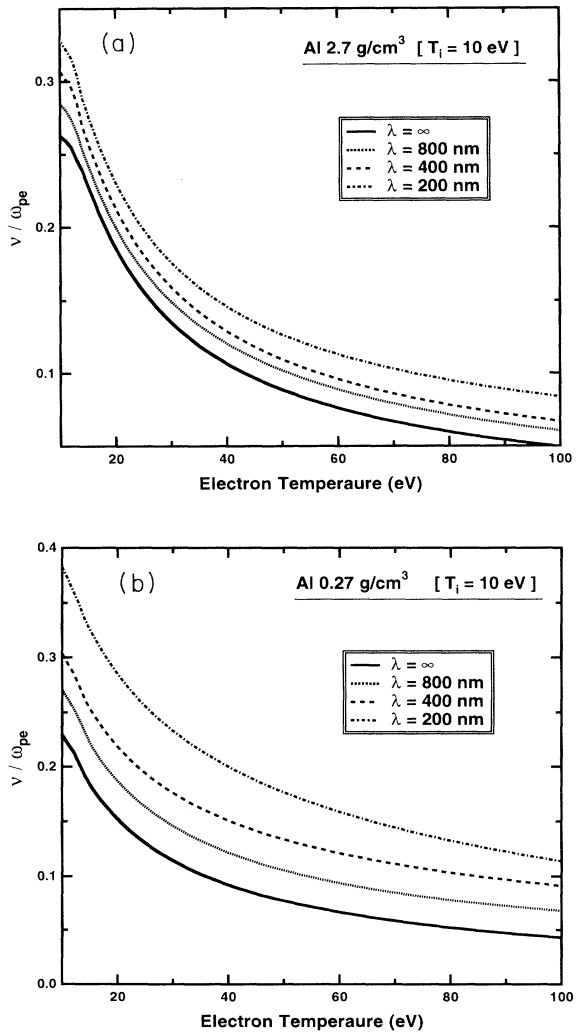


FIG. 5. (a) The two-temperature ac electron-ion collision frequency $\nu(\omega)$ in units of the electron plasma frequency for solid density aluminum for selected wavelengths. The ion temperature is fixed at 10 eV. (b) Same as (a) but for one-tenth-solid density aluminum.

## ACKNOWLEDGMENTS

This work was supported by Lawrence Livermore National Laboratory under the auspices of the U.S. Department of Energy under Contract No. W-7405-ENG-48 and by the Natural Sciences and Engineering Research Council of Canada (NSERC).

## APPENDIX: MOMENTUM STATES

This appendix contains the definitions of the momentum states used in the solution of Eq. (5). The five hydrodynamic momentum states can be defined [16] by

$$
\begin{aligned}
H_n^{\alpha_1} &= 1/(n_{\alpha_1})^{1/2} , \\
H_{px}^{\alpha_1} &= p_x/(n_{\alpha_1} m_{\alpha_1} T_{\alpha_1})^{1/2} , \\
H_{py}^{\alpha_1} &= p_y/(n_{\alpha_1} m_{\alpha_1} T_{\alpha_1})^{1/2} , \\
H_{pz}^{\alpha_1} &= p_z/(n_{\alpha_1} m_{\alpha_1} T_{\alpha_1})^{1/2} , \\
H_{\epsilon}^{\alpha_1} &= (\vec{p}^2/m_{\alpha_1} T_{\alpha_1} - 3)/(6 n_{\alpha_1})^{1/2} .
\end{aligned}
\tag{A1}
$$

The hydrodynamic subspace projection operator $P$ is then

$$
P = \sum_{\alpha=e,i} \sum_{j=1}^{5} |H_j^{\alpha}\rangle\langle H_j^{\alpha}| . \tag{A2}
$$

For electrical resistivity, only vector moments contribute

(cf. [7,14]). They consist of one of the three momentum components $H^{\alpha_1}_{p\gamma}(\gamma=x,y,z)$ (A1) and some of the nonhydrodynamic states. Since our model approximates the electrical resistivity with accuracy to zero order terms in mass ratio $m_e/m_i$, only electron moments are taken into account. The first nonhydrodynamic vector set of electron momentum states, describing heat conduction, is given by

$$H^e_{q\gamma}=(1/10n_e)^{1/2}[p_\gamma/(m_eT_e)]^{1/2}(\vec{p}^2/m_eT_e-5)\ , \quad \text{(A3)}$$

where $\gamma$ is an index representing the three spatial directions. The next set of contributing states, fifth order vector momentum states, are

$$H^e_{r_\gamma}=(1/280n_e)^{1/2}[p_\gamma/(m_eT_e)]^{1/2} \times[\vec{p}^4/(m_eT_e)^2-14\vec{p}^2/m_eT_e+35]\ , \quad \text{(A4)}$$

where $\gamma=x,y,z$. Our definition of $Q$ is

$$Q\approx\sum_{\gamma=x,y,z}(|H^e_{q_\gamma}\rangle\langle H^e_{q_\gamma}|+|H^e_{r_\gamma}\rangle\langle H^e_{r_\gamma}|)\ . \quad \text{(A5)}$$

The operator $iQ\Phi^CQ$ in Eq. (7) can then be built from a two-dimensional representation

$$iQ\Phi^CQ=\sum_{\eta_1,\eta_2=q_\gamma,r_\gamma}|H^e_{\eta_1}\rangle M_{\eta_1\eta_2}\langle H^e_{\eta_2}|\ , \quad \text{(A6)}$$

where the matrix elements are defined by

$$M_{\eta_1\eta_2}=\langle H^e_{\eta_2}|i\Phi^C|H^e_{\eta_1}\rangle\ . \quad \text{(A7)}$$

The matrix elements are

$$\begin{aligned}
M_{pp}&=A\tfrac{1}{6}\beta_{ei}^{1/2}\Delta\ ,\\
M_{rr}&=A\left[\frac{3\sqrt{2}Z}{28}\beta_e^{1/2}\Omega^{ee}+\frac{433}{1680}\beta_{ei}^{1/2}\Omega^{ei}\right]\ ,\\
M_{qq}&=A\left[\frac{\sqrt{2}Z}{15}\beta_e^{1/2}\Omega^{ee}+\frac{13}{60}\beta_{ei}^{1/2}\Omega^{ei}\right]\ ,\\
M_{qr}&=-A\left[\frac{Z}{5\sqrt{14}}\beta_e^{1/2}\Omega^{ee}+\frac{23}{20\sqrt{28}}\beta_{ei}^{1/2}\Omega^{ei}\right]\ ,\\
M_{pq}&=-A\frac{\sqrt{2}}{8\sqrt{5}}\beta_{ei}^{1/2}(\Delta+\Omega^{ei})\ ,\\
M_{pr}&=A\frac{5\sqrt{2}}{16\sqrt{35}}\beta_{ei}^{1/2}(\Delta+\Omega^{ei})\ ,
\end{aligned} \quad \text{(A8)}$$

where $A=n_i/\pi\sqrt{2\pi m_e}$, $\beta_\alpha=1/T_\alpha$, $\beta_{\alpha_1\alpha_2}=1/T_{\alpha_1\alpha_2}$, and

$$T_{\alpha_1\alpha_2}=\frac{m_{\alpha_1}T_{\alpha_2}+m_{\alpha_2}T_{\alpha_1}}{m_{\alpha_1}+m_{\alpha_2}}\ .$$


[1] M. M. Murname, H. C. Kapteyn, and R. W. Falcone, Phys. Rev. Lett. **62**, 155 (1989); H. M. Milchberg, R. R. Freeman, S. C. Davey, and R. M. More, *ibid.* **61**, 2364 (1988); J. C. Kieffer, P. Audebert, M. Chaker, J. P. Matte, H. Pepin, T. W. Johnston, P. Maine, D. Meyerhofer, J. Delletrez, D. Strickland, P. Bado, and G. Mourou, *ibid.* **62**, 760 (1989); R. Fedosejevs, R. Ottman, R. Siegel, G. Kuhnle, S. Szatmari, and F. P. Schafer, *ibid.* **64**, 1250 (1990).

[2] R. Cauble, F. J. Rogers, and W. Rozmus, in *Strongly Coupled Plasma Physics,* edited by S. Ichimaru (Elsevier, New York, 1990), p. 439.

[3] R. M. More, Z. Zinamon, K. H. Warren, R. Falcone, and M. Murnane, J. Phys. (Paris) **49**, C7-43 (1988).

[4] R. Shepherd, R. Booth, D. Price, R. Walling, R. More, G. Guethlein, B. Young, J. Dunn, A. Osterheld, W. Goldstein, and R. Stewart, in *Laser Interaction and Related Plasma Phenomena,* 11th International Workshop, edited by George H. Miley, AIP Conf. Proc. 318 (AIP, New York, 1994), p. 30.

[5] M. W. C. Dharma-wardana and F. Perrot, Phys. Lett. A **163**, 223 (1992).

[6] A. Ng, P. Celliers, A. Forsman, R. M. More, Y. T. Lee, F. Perrot, M. W. C. Dharma-wardana, and G. A. Rinker, Phys. Rev. Lett. **72**, 3351 (1994).

[7] R. Cauble and W. Rozmus, J. Plasma Phys. **37**, 405 (1987).

[8] W. Rozmus and R. Cauble, Phys. Lett. A **112**, 440 (1985).

[9] R. Cauble and W. Rozmus, Phys. Fluids **28**, 3387 (1985).

[10] A. N. Mostovych, K. J. Kearney, J. A. Stamper, and A. J. Schmitt, Phys. Rev. Lett. **66**, 612 (1991).

[11] J. P. Hansen and I. R. MacDonald, Phys. Rev. A **23**, 2041 (1979).

[12] G. F. Mazenko, Phys. Rev. A **9**, 360 (1974).

[13] J. Wallenborn and M. Baus, Phys. Rev. A **18**, 1737 (1978).

[14] R. Balescu, *Transport Processes in Plasmas* (North-Holland, Amsterdam, 1988), Vol. 1.

[15] D. Forster and P. C. Martin, Phys. Rev. A **2**, 1515 (1970).

[16] M. Baus, Physica A **88**, 319 (1977); **88**, 336 (1988).

[17] H. Grad, Commun. Pure Appl. Math. **2**, 311 (1949).

[18] S. I. Braginskii, in *Reviews of Plasma Physics,* edited by M. A. Leontovich (Consultants Bureau, New York, 1965), p. 205.

[19] D. B. Boercker, F. J. Rogers, and H. E. DeWitt, Phys. Rev. A **25**, 1623 (1982).

[20] P. Seuferling, J. Vogel, and C. Toepffer, Phys. Rev. A **40**, 323 (1989).

[21] C. Deutsch, Phys. Lett. A **60**, 317 (1977); C. Deutsch, M. M. Gombert, and H. Minoo, *ibid.* **72**, 481 (1979).

[22] R. Cauble and W. Rozmus (unpublished).

[23] Y. T. Lee and R. M. More, Phys. Fluids **27**, 1273 (1984).

[24] L. Spitzer, *Physics of Fully Ionized Gases,* 2nd ed. (Interscience, New York, 1962).

[25] Naval Research Laboratory Report No. NRL-PU-6790-94-265, 1994 (unpublished).

[26] R. M. More (unpublished).

[27] D. F. Price *et al.*, Phys. Rev. Lett. **75**, 252 (1995).